HTML ABSTRACT + LINKS

Thermal expansion of Ti-containing hydrogenated amorphous carbon nanocomposite thin films

B. Shi and W. J. Meng[a)]
Mechanical Engineering Department, Louisiana State University, Baton Rouge, Louisiana 70803

T. L. Daulton
Naval Research Laboratory, Marine Geosciences Division, Stennis Space Center, Mississippi 39529

(Received 12 July 2004; accepted 16 September 2004)

The effective coefficients of thermal expansion (CTE) of Ti-containing hydrogenated amorphous carbon (Ti–C:H) thin films were measured. Ti–C:H thin films with compositions ranging from nearly pure *a*-C:H to nearly pure TiC were deposited on Si(100) substrates. Effective CTEs were determined from temperature induced changes in the curvature of film/substrate assemblies. Measured effective CTE values for Ti–C:H are $\sim 5.7\times 10^{-6}$ K^{-1}, and show little dependence on the Ti composition. © *2004 American Institute of Physics*. [DOI: 10.1063/1.1814800]

Coefficients of thermal expansion (CTE) of hydrogenated amorphous carbon (*a*-C:H) thin films has been measured previously.[1] However, little is known about the CTE of *a*-C:H films containing more than a few atomic percent of carbide forming metals (Me–C:H). While *a*-C:H films are homogeneous on length scales larger than a few nanometers, Me–C:H films are nanocomposites with metal–carbide nanocrystals embedded within *a*-C:H.[2] Ti–C:H thin films consist of B1–TiC nanoclusters embedded within *a*-C:H.[3] Due to the orientational isotropy of *a*-C:H and the cubic symmetry of B1–TiC, the CTEs of both phases are represented by scalar quantities.[4] In this paper, effective CTEs of Ti–C:H thin films are measured as a function of the Ti composition.

Ti–C:H thin films were synthesized with an inductively coupled plasma assisted hybrid chemical/physical vapor deposition technique.[5] A series of Ti–C:H thin films were deposited onto the front sides of two-side polished, 300 μm-thick Si(100) substrates, cut along ⟨100⟩ directions into 4×30 mm beams. The substrate curvature change due to Ti–C:H deposition were measured *in situ* with a multibeam optical sensing (MBOS) technique.[6] Each Ti–C:H specimen was deposited in the configuration of Ti–C:H/Ti/Si(100) with a ~80 nm-thick Ti interlayer, and a Ti–C:H layer thickness of 1–2 μm. Substrate temperatures during Ti–C:H deposition were ~250 °C. The Ti to C atomic ratio ($R_{\mathrm{Ti/C}}$) was obtained from Rutherford backscattering spectrometry measurements.[6]

Carbon *K*-edge electron energy-loss spectroscopy (EELS) measurements on plan-view Ti-C:H specimens were performed on a JEOL JSM3010 transmission electron microscope operated at 300 kV and equipped with a Gatan imaging filter (GIF200). Raman scattering spectra were collected at room temperature in reflection from as-deposited Ti–C:H/Ti/Si(100) specimens with a Jobin–Yvon Horiba LabRam instrument.

The effective CTEs of Ti–C:H films were probed by measuring the specimen curvature change with the MBOS technique during heating induced temperature excursions. Because of the large thickness disparity between the Ti–C:H and Ti layers, the thermal expansion of the latter was neglected. The beam assembly was clamped on one end onto a specimen holder with the other end free, and placed in the center of a high vacuum tube furnace. The tube furnace was sealed at one end with an optical quality glass allowing laser beam access, and evacuated to a base pressure of $\sim 2\times 10^{-8}$ Torr. The specimen temperature was monitored by a *K*-type thermocouple placed 3 mm away from the beam assembly. During each CTE measurement cycle, the specimen temperature was increased over ~120 min from room temperature to <230 °C, followed by a similarly slow decrease to room temperature. A linear array of parallel laser beams were incident on the film side of the specimen assembly, and the reflected spots were detected by a charge-coupled-device (CCD) array. The curvature of the beam assembly, *K*, is related to the relative change in spacing between reflected spots, by

$$K = -\left(\frac{D - D_0}{D_0}\right)\frac{\cos\theta}{2L}, \tag{1}$$

where D is the reflected spot spacing from a specimen with curvature K, and θ, L, and D_0 are, respectively, the incidence angle, the optical path length from the specimen to the CCD, and the spacing between reflected spots from a *flat* surface. In the present setup, L was 163 cm and θ was ~1°. A negative change in K denotes increasing substrate convexity on the film side.

When the film/substrate assembly is subjected to a temperature change, ΔT, the thermal stress generated within the film, σ_f, due to the mismatch between the CTE of the Si substrate, α_s, and the effective CTE of the Ti–C:H film, α_f, is given by

$$\sigma_f = -\frac{E_f}{1-\nu_f}(\alpha_f - \alpha_s)\Delta T. \tag{2}$$

This thermal stress induces a change in curvature, ΔK, of the film/substrate assembly according to the Stoney's equation

$$\sigma_f t_f = \frac{1}{6}t_s^2\left(\frac{E_s}{1-\nu_s}\right)\Delta K, \tag{3}$$

where t_f and t_s are the thicknesses of film and substrate, respectively. In Eqs. (2) and (3), $E_f/(1-\nu_f)$ and $E_s/(1-\nu_s)$

[a)]Electronic mail: wmeng@me.lsu.edu

 © 2004 American Institute of Physics

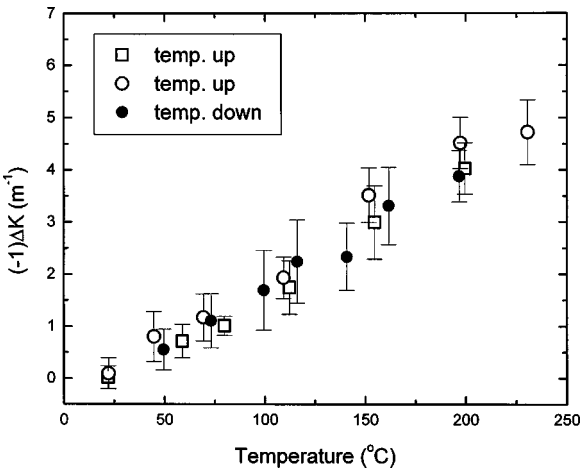

FIG. 1. Measured curvature change of a Ti–C:H/Ti/Si(100) beam assembly as a function of temperature. Open and solid circles denote results measured during temperature rise and fall of one continuous temperature excursion over a ~300 min period. Open squares denote data obtained during a separate temperature rise 24 h later.

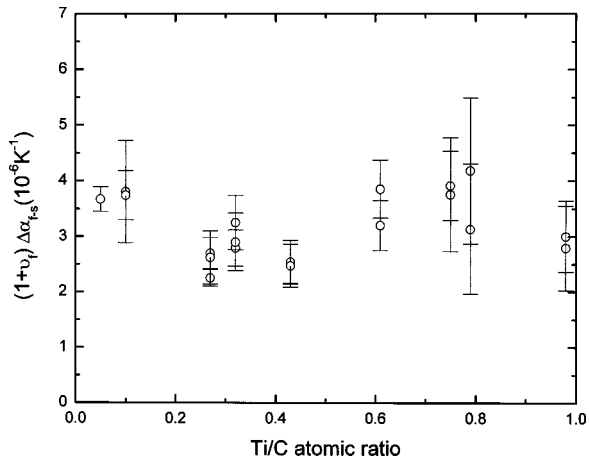

FIG. 2. Measured CTE mismatch between Ti–C:H and Si as a function of the Ti composition. The use of the film indentation modulus instead of the biaxial modulus results in an additional factor of $(1+\nu_f)$. Separate data points at the same $R_{\mathrm{Ti/C}}$ denote results of repeat measurements on the same specimen.

are, respectively, the biaxial moduli of the film and substrate.

The CTE mismatch, $\Delta\alpha_{f-s} \equiv \alpha_f - \alpha_s$, is obtained from Eqs. (2) and (3), and is a function of $\Delta K/\Delta T$ as well as the biaxial moduli and thicknesses of both the film and substrate. For the present measurements, $E_s/(1-\nu_s) = 1.805\times 10^{11}$ Pa,[7] $t_s = 300$ μm, and t_f was directly measured. Although $E_f/(1-\nu_f)$ values for Ti–C:H films were not measured, their indentation moduli, $E_{\mathrm{ind}} = E_f/(1-\nu_f^2)$, were determined previously from instrumented nanoindentation measurements.[8] The knowledge of E_{ind} allowed one to determine $(1+\nu_f)\Delta\alpha_{f-s}$:

$$(1+\nu_f)\Delta\alpha_{f-s} = -\frac{1}{6}\frac{t_s^2}{t_f}\left(\frac{E_s}{1-\nu_s}\right)\frac{1}{E_{\mathrm{ind}}}\frac{\Delta K}{\Delta T}. \tag{4}$$

If $\Delta\alpha_{f-s}$ is independent of temperature in the temperature excursion range, then ΔK is linearly proportional to ΔT.

Because of the presence of compressive intrinsic stresses within Ti–C:H, ranging from 0.5 to 2 GPa in magnitude,[6] and the absence of stress relaxation,[8] as-deposited Ti–C:H/Ti/Si(100) film/substrate assemblies possessed significant curvatures. Because of this initial curvature, one caveat exists regarding the ΔK measurements. Applying Eq. (1), one obtains

$$\Delta K = K_2 - K_1 = -\left(\frac{\cos\theta}{2L}\right)\frac{D_2 - D_1}{D_0}$$
$$= -\left(\frac{\cos\theta}{2L}\right)\left(\frac{D_2 - D_1}{D_1}\right)\left(1 + \frac{D_1 - D_0}{D_0}\right), \tag{5}$$

where D_1 is the reflected spot spacing at the beginning of the temperature excursion, corresponding to the curvature K_1 of the as-deposited film/substrate assembly. The last term in Eq. (5) is usually insignificant for bare substrates. In the present case, it is substantially different from unity. However, it is known from previous substrate curvature measurements during specimen deposition,[6] and was applied to obtained $\Delta K(T)$.

Structural stability of the Ti–C:H films during the temperature excursion is of concern, since the CTE measurements assumes that thermally induced strains are elastic in origin, and excludes any structural changes within Ti–C:H. Figure 1 shows measured ΔK as a function of temperature for a Ti–C:H/Ti/Si(100) beam assembly, in which the Ti–C:H film has $R_{\mathrm{Ti/C}} \sim 0.43$. As the temperature increases, ΔK becomes more negative, indicating that $\alpha_f > \alpha_s$. Results of three separate ΔK measurements are shown, and show that, within experimental error, the thermally induced ΔK is reproducible over repeated temperature excursions up to ~230 °C and linearly proportional to ΔT. The former suggests that no structural modification occurred within the film during the measurement.

Measured values of $(1+\nu_f)\Delta\alpha_{f-s}$ for Ti–C:H as a function of the Ti composition are shown in Fig. 2. The reported error bars are derived from measurement errors in ΔK, t_f, and E_{ind}, and are dominated by scatter in the E_{ind} measurement.[8] Data shown in Fig. 2 indicate that $(1+\nu_f)\Delta\alpha_{f-s}$ approaches $\sim 3.5\times 10^{-6}$ K^{-1} and $\sim 3.0\times 10^{-6}$ K^{-1} as $R_{\mathrm{Ti/C}}$ approaches, respectively, 0 or 1, and shows only marginal variation outside of measurement error as a function of the Ti composition.

The bonding configuration of the *a*-C:H phase in Ti–C:H was further probed by EELS[9] and Raman scattering.[10] Figure 3 shows a C *K*-edge EELS spectrum col-

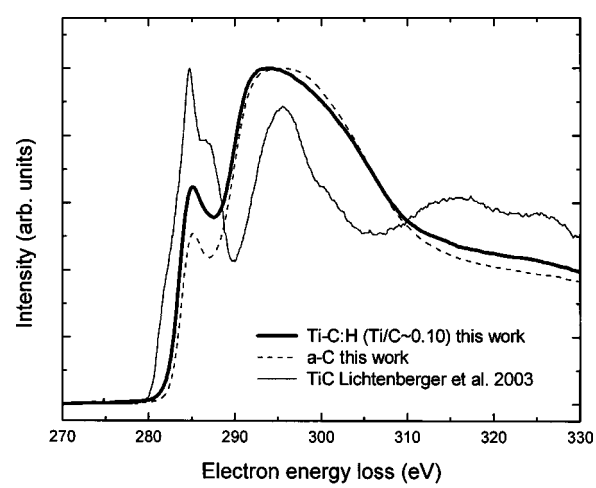

FIG. 3. Probing the bonding configuration of the *a*-C:H phase within Ti–C:H: C *K*-edge EELS spectra of a Ti–C:H thin film with $R_{\mathrm{Ti/C}} = 0.10$, an evaporated amorphous carbon (*a*-C) film, and TiC (see Ref. 11). Note that the π^* peak for Ti–C:H is stronger relative to that for a-C.

lected from a Ti–C:H film with $R_{Ti/C} \sim 0.10$. The intensity of the 1s-π^* peak near 285 eV relative to the C *K*-edge as a whole is proportional to the fraction of sp^2 bonded C atoms, f_{sp^2}.[9] Quantitative evaluation of f_{sp^2} in this case is complicated by the presence of the TiC phase within Ti–C:H. Although TiC contains no sp^2 bonded C, it displays a strong EELS peak near 285 eV relative to the C *K*-edge.[11] Adding the C *K*-edge signal from TiC to that of *a*-C:H can result in a spectral distortion, and the composite spectra is no longer reflective of the true sp^2 C component.

A number of Raman spectra were obtained from Ti–C:H specimens with different Ti contents. At all Ti compositions, Raman spectra contained the *D* and *G* bands commonly observed in *a*-C:H films. The *D* band center is located at 1368–1375 cm^{-1}, with its full width at half maximum (FWHM) ranging from 296 to 303 cm^{-1}. The *G* band center is located at 1551–1557 cm^{-1}, with its FWHM ranging from 108 to 130 cm^{-1}. As $R_{Ti/C}$ increases from 0.02 to 0.17, the *D* and *G* band positions and their FWHMs do not change significantly. The band heights, however, decrease by approximately a factor of 5. The similarity in Raman spectral shapes observed from Ti–C:H specimens with different $R_{Ti/C}$ suggests that the structure of the *a*-C:H phase within Ti–C:H does not change significantly as the Ti composition changes. Previous x-ray absorption spectroscopy measurements on Ti–C:H thin films showed that the bonding environment surrounding Ti atoms is similar to that in bulk TiC.[3] These observations suggest that the structure of the TiC phase within Ti–C:H is likewise not significantly modified as $R_{Ti/C}$ varies.

Since the structures of the *a*-C:H and TiC phases within Ti–C:H show no strong evidence of being modified from their corresponding pure forms, $\Delta\alpha_{f-s}$ can be approximated, to first order, from Eq. (4) using the Poisson's ratio of bulk TiC (υ=0.17)[12] and pure *a*-C:H ($\upsilon \sim 0.3$, independent of f_{sp^2}).[1] Using those values for υ_f yields $\Delta\alpha_{f-s}=2.7 \times 10^{-6}$ K^{-1} and 2.6×10^{-6} K^{-1} for Ti–C:H at compositions approaching respectively pure *a*-C:H and pure TiC. As temperature increases from 300 to 500 K, α_s increases from 2.6×10^{-6} K^{-1} to 3.6×10^{-6} K^{-1}.[13] Taking the average value of $\alpha_s=3.1\times10^{-6}$ K^{-1}, the data shown in Fig. 2 yields effective CTE values for Ti–C:H, in the temperature interval of 300–500 K, of 5.8×10^{-6} K^{-1} (nearly pure *a*-C:H) and 5.7×10^{-6} K^{-1} (nearly pure TiC). According to Marques *et al.*, a CTE value of 5.8×10^{-6} K^{-1} for *a*-C:H corresponds to $f_{sp^2}\approx0.8$.[1] Given the low Ti content ($R_{Ti/C}\sim0.10$) of the Ti–C:H film examined by EELS, qualitative comparison between the EELS data shown in Fig. 3 and previous EELS data on amorphous carbon films with varying sp^2 C content[14] suggests a high f_{sp^2} value in the *a*-C:H phase. Moreover, Weiler *et al.* reported a relationship between intrinsic stress within *a*-C:H films and f_{sp^2}. They demonstrated that a compressive intrinsic stress of ~2 GPa (as measured for our Ti–C:H films at compositions approaching pure *a*-C:H)[6] corresponds to a f_{sp^2} of ~0.8.[15]

The presently determined effective CTE for the TiC phase within Ti–C:H is, however, lower than the value of 7.0×10^{-6} K^{-1} for bulk TiC.[16] Likewise, the measured E_{ind} value of ~250 GPa for Ti–C:H films with composition approaching pure TiC is significantly below the corresponding value for bulk TiC.[12] This suggests that the CTE and E_{ind} of single-phase TiC can be significantly altered by forming a TiC/*a*-C:H nanocomposite with only a minor fraction of *a*-C:H.

To obtain CTE for Ti–C:H, one needs to consider the variation of the Poisson's ratio υ of Ti–C:H as the Ti composition varies. Variations of υ in two-phase composites have been analyzed from a continuum mechanics view point. Simple analysis for long-fiber composites indicates a linear rule-of-mixtures variation.[17] Effective medium theory analysis of random two-phase composites, in which the two phases have identical Poisson's ratios, has shown that the composite υ exhibits no pronounced variation with composition when υ values of the component phases range from 0.1 to 0.4.[18] Within the average relative error of ~18% for the data shown in Fig. 2, the present measurements indicate that the effective CTE of Ti–C:H is $\sim5.7\times10^{-6}$ K^{-1} and essentially independent of the Ti composition, regardless of whether υ is taken to be 0.3, 0.17, or the linear rule-of-mixtures values. The lack of composition dependence of measured effective CTE for Ti–C:H is expected from continuum mechanics, based on the near equality of CTEs for nearly pure *a*-C:H and TiC.[19] Since an abundance of TiC/*a*-C:H interfaces exists within Ti–C:H, our measurements suggest that these interfaces do not exert any anomalous influence over the average thermal expansion behavior of these nanocomposites.

W.J.M. and B.S. acknowledge partial project support from NIST ATP 70NANBH0H3048 through a subcontract with Caterpillar Inc., NSF through Grant Nos. DMI-0124441 and DMI-0400061, and Louisiana Board of Regents through Contract Nos. LEQSF(2001-04)-RD-A-07 and LEQSF(2004-07)-RD-B-06. Technical assistance by R. D. Evans of Timken Research in Raman experimentation is acknowledged with thanks.

[1] F. C. Marques, R. G. Lacerda, A. Champi, V. Stolojan, D. C. Cox, and S. R. P. Silva, Appl. Phys. Lett. **83**, 3099 (2003).
[2] W. J. Meng and B. A. Gillispie, J. Appl. Phys. **84**, 4314 (1998).
[3] W. J. Meng, R. C. Tittsworth, J. C. Jiang, B. Feng, D. M. Cao, K. Winkler, and V. Palshin, J. Appl. Phys. **88**, 2415 (2000).
[4] J. F. Nye, *Physical Properties of Crystals, Their Representation by Tensors and Matrices* (Clarendon, Oxford 2001).
[5] W. J. Meng, E. I. Meletis, L. E. Rehn, and P. M. Baldo, J. Appl. Phys. **87**, 2840 (2000).
[6] B. Shi, W. J. Meng, L. E. Rehn, and P. M. Baldo, Appl. Phys. Lett. **81**, 352 (2002).
[7] W. A. Brantley, J. Appl. Phys. **44**, 534 (1973).
[8] B. Shi and W. J. Meng, J. Appl. Phys. **94**, 186 (2003).
[9] S. D. Berger, D. R. McKenzie, and P. J. Martin, Philos. Mag. Lett. **57**, 285 (1988).
[10] A. C. Ferrari and J. Robertson, Phys. Rev. B **61**, 14095 (2000).
[11] O. Lichtenberger, E. Pippel, J. Woltersdorf, and R. Riedel, Mater. Chem. Phys. **81**, 195 (2003).
[12] L. E. Toth, *Transition Metal Carbides and Nitrides* (Academic, New York, 1971).
[13] M. Okaji, Int. J. Thermophys. **9**, 1101 (1988).
[14] D. G. McCulloch, E. G. Gerstner, D. R. McKenzie, S. Prawer, and R. Kalish, Phys. Rev. B **52**, 850 (1995).
[15] M. Weiler, S. Sattel, T. Giessen, K. Jung, H. Ehrhardt, V. S. Veerasamy, and J. Robertson, Phys. Rev. B **53**, 1594 (1996).
[16] R. O. Elliott and C. P. Kempter, J. Phys. Chem. **62**, 630 (1958).
[17] D. Hull and T. W. Clyne, *An Introduction to Composite Materials* (Cambridge University Press, Cambridge, 1996).
[18] E. J. Garboczi and A. R. Day, J. Mech. Phys. Solids **43**, 1349 (1995).
[19] C. H. Hsueh, P. F. Becher, and E. Y. Sun, J. Mater. Sci. **36**, 255 (2001).